Electrical and optical properties of carbon-doped GaSb

R. D. Wiersma, J. A. H. Stotz, O. J. Pitts, C. X. Wang, M. L. W. Thewalt,
and S. P. Watkins*
Department of Physics, Simon Fraser University, Burnaby, British Columbia, V5A 1S6, Canada
(Received 16 April 2002; revised manuscript received 14 January 2003; published 16 April 2003)

We report low-temperature Hall-effect and photoluminescence measurements on samples of GaSb lightly doped with carbon in the range of 10^{16}– 5×10^{17} cm^{-3}. Temperature, excitation intensity, and impurity concentration dependent photoluminescence (PL) measurements were used to determine a shallow acceptor binding energy for carbon in GaSb of 12.9 ± 1 meV. The carbon acceptor PL transition was determined to be due to a combination of donor-acceptor pair and free-to-bound processes. Temperature-dependent Hall-effect analysis of hole concentration and mobility were performed on nominally undoped and lightly carbon-doped epilayers and on bulk undoped Czochralski-grown GaSb. Experimental hole concentrations of the carbon-doped epilayers were fitted to a two acceptor model that included the deep native acceptor and shallow carbon acceptor levels. Activation energies of 8–11 meV were determined for the lightest carbon-doped samples through least-squares fitting of the experimental hole concentration versus temperature. Carbon-doped epilayers showed significantly higher impurity band conduction at low temperatures than Czochralski-grown GaSb due to the shallower nature of the carbon acceptor levels. Hall mobility data confirmed the presence of impurity band conduction below 10 K, in addition to the usual scattering mechanisms.

DOI: 10.1103/PhysRevB.67.165202 PACS number(s): 72.20.−i, 78.55.−m

I. INTRODUCTION

Carbon-doped GaAsSb has received increased interest due to its recent use as the base layer in high-speed heterojunction bipolar transistors.[1] The small band gap of antimony-based materials makes them suitable candidates for long-wavelength emitters and detectors in the 2–5-μm range.[2] Carbon is an effective *p*-type dopant for certain III–V compounds such as GaAs and AlGaAs due to its small diffusion coefficient, high solubility, and the fact that high concentrations and abrupt doping profiles can be obtained.[3,4] Very little information has been reported on the use of carbon as a dopant source for GaSb.[5–7] Baldereschi and Lipari have used effective-mass approximation calculations for shallow acceptor states in cubic semiconductors to predict an acceptor binding energy of 12.5 meV for GaSb.[8] There have been several reports in the literature of shallow acceptor levels in GaSb. Far-infrared absorption studies on Si-doped GaSb have reported spectroscopic acceptor binding energies ranging from 13–15 meV that seem to confirm the effective-mass prediction.[9] Jakowetz *et al.* investigated Si and Ge doping of GaSb grown by liquid phase epitaxy (LPE).[10] Through PL studies they reported transitions at $\approx$800 meV that they attributed to donor-acceptor pair (DAP) recombination. Acceptor binding energies of 9.4 meV for Si and 9.5 meV for Ge were obtained. The discrepancy between the experimentally determined shallow acceptor binding energies of Jakowetz *et al.* and the effective-mass value could be due to improper identification of the PL transition. Considering the luminescence as a band-to-acceptor or free-to-bound (FB) transition would increase the energy by approximately 2–3 meV, resulting in values near the values predicted by Baldereschi and Lipari. Hjelt and Tuomi have investigated organometallic vapor phase epitaxy (OMVPE) grown GaSb on GaAs substrates doped with Zn.[11] They reported a band-to-zinc acceptor transition of 13 meV that is in close agreement with theory. However, these authors did not take into account lattice induced strain between the GaAs substrate and GaSb epilayer that can affect the estimation of the acceptor binding energy.

GaSb contains a doubly ionizable native defect due to Ga vacancies (V_{Ga}) paired with Ga on Sb (Ga_{Sb}) antisite defects. This V_{Ga}-Ga_{Sb} defect leads to an intrinsic hole concentration that is influenced by the growth method. Melt grown material usually has room-temperature hole concentrations greater than 10^{17} cm^{-3} whereas the lowest hole concentrations, obtained with molecular-beam epitaxy (MBE), are somewhat greater than 10^{15} cm^{-3}.[12] The native acceptor binding energies for the single and double ionizable acceptor states as determined from PL studies are in the range of 33–36 meV and 102–103 meV, respectively.[13,14] In a previous work,[5] we reported the use of carbon tetrachloride as a *p*-type dopant for GaSb. Doping levels from 10^{16} to 10^{20} cm^{-3} were obtained. In lightly carbon-doped samples grown on GaAs substrates we observed a carbon related shallow acceptor peak by PL.

In the present work, we have produced similarly carbon-doped samples grown on GaSb substrates in order to eliminate strain shifts and broadening in the PL features. We report detailed temperature-dependent PL analysis and the effect of excitation intensity and doping level, in order to clarify the physical origin of the shallow carbon related luminescence features, and thereby extract an estimate of the carbon acceptor binding energy. In addition we performed detailed temperature-dependent Hall-effect measurements on samples grown under similar conditions on GaAs substrates, and show that the presence of shallow carbon acceptors brings about large changes in the transport properties, despite having a lower concentration than the deep level native defect. The data show a two band conduction behavior in which conduction at higher temperatures is dominated by free holes in the valence band, while at low temperatures

 ©2003 The American Physical Society

conduction is dominated by a low mobility impurity band due to the overlap of the acceptor ground states.[15]

II. EXPERIMENT

The substrates used for the growth of the GaSb epilayers were GaAs (001) (AXT, semi-insulating) and GaSb (001) (Ramet, Te doped, 10^{18} cm^{-3}). All growths were carried out in a vertical chamber Thomas Swan OMVPE reactor. Palladium diffused hydrogen at a flow rate of 2.3 L/min was used as the carrier gas. The reactor pressure for all growths was 100 Torr. Source materials were trimethylgallium (TEGa, partial pressure: 1.7×10^{-2} Torr) and triethylantimony (TMSb, partial pressure: 2.6×10^{-2} Torr). The dopant source was carbon tetrachloride (CCl_4, 500 ppm in hydrogen).

For growth on GaAs substrates a low-temperature buffer layer of 300 Å grown at 400 °C was necessary before increasing the temperature to 560 °C for the thick epilayer growth. Growth on GaSb substrates was performed using the same conditions as used for the GaAs substrates but with the removal of the low-temperature buffer layer. In both cases the optimal V/III ratio was found to be approximately 1.5. Below this ratio Ga droplets formed and above this ratio the surface became polycrystalline.

High-resolution x-ray diffraction (HRXRD) was used to determine epilayer thickness and growth rates. The HRXRD system consists of a Cu anode source and a Bede D3 triple axis diffractometer with asymmetrically cut Si (022) crystal beam conditioner and analyzer crystals.

The van der Pauw technique was used to obtain Hall-effect measurements of the carrier concentration and mobility of carbon-doped GaSb on GaAs substrates. An In-Zn alloy was used to make electrical contacts by heating the sample under hydrogen gas to 300 °C. A Janis varitemp liquid-He cryostat in conjunction with a controlled electrical heater was used for temperature-dependent Hall-effect measurements between 4.2 and 320 K. A Hall factor of unity was assumed throughout.

For PL experiments, samples were mounted strain free in a liquid-He cryostat. The temperature was monitored with a calibrated diode. A multiline, continuous-wave argon ion laser was used for the PL excitation, at power densities between 0.01 W/cm^2 and 10 W/cm^2. For the temperature-dependent spectra, optical excitation was kept to a minimum to reduce the heat load on the sample. Spectral analysis was performed using a Bomem DA8 Fourier transform interferometer with a North Coast liquid-nitrogen-cooled germanium photodiode. Reflection spectra were obtained using a quartz-halogen white light source and a room-temperature InGaAs detector together with the DA8.

III. RESULTS AND DISCUSSION

A. Hall analysis

Temperature-dependent Hall-effect measurements were performed on samples varying in hole concentration from $p_{300}=5.0\times10^{16}$ cm^{-3} to $p_{300}=5.8\times10^{17}$ cm^{-3}. A plot of hole concentration as a function of reciprocal temperature is displayed in Fig. 1 for undoped and carbon-doped samples of

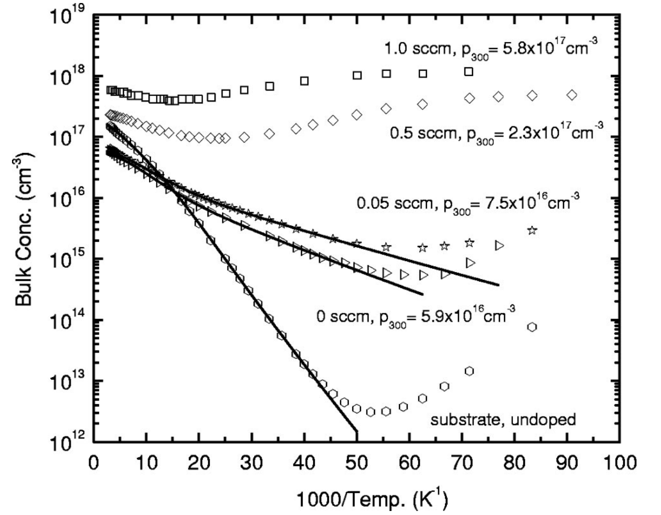

FIG. 1. Temperature-dependent free-carrier concentrations for undoped and lightly carbon doped GaSb samples. Carrier concentration freezeout is shown as samples are cooled from 320 K to approximately 10 K. The onset of impurity band conduction is indicated by the increase in free-carrier concentration at lower temperatures.

GaSb. The amount of freezeout varies significantly between the undoped GaSb substrate and the lightly carbon-doped or undoped GaSb epilayers. At very low temperatures, the apparent hole concentration begins to increase due to the onset of impurity band conduction caused by the banding of the $1s$ acceptor ground states.[15] This impurity band conduction effect is stronger for more heavily doped samples as can be clearly seen in Fig. 1. In the temperature range in which valence band conduction dominates, fits to the hole concentration data were made assuming a compensated two-acceptor model:

$$p=\frac{N_{carbon}}{1+\frac{gp}{N_V}\exp(E_{carbon}/kT)}+\frac{N_{native}}{1+\frac{gp}{N_V}\exp(E_{native1}/kT)}-N_D, \quad (1)$$

where N_{carbon} is the total density of carbon impurities, N_{native} is the density of the native defect, E_F is the Fermi energy, E_{carbon} is the acceptor binding energy of carbon, and $E_{native1}$ is the first acceptor binding energy of the native defect. The valence-band degeneracy factor g is assumed to be equal to 4. The native acceptor energy determined by PL was used as an upper constraint on $E_{native1}$ of $\leqslant$33 meV. The Fermi energy is given by

$$E_F=E_v-kT\ln\left(\frac{p}{N_v}\right), \quad (2)$$

where E_v is the energy of the valence band and N_v is the thermal average density of states of the valence band. Using the effective masses of the heavy and light holes ($m_{hh}=0.4m_0$, $m_{lh}=0.05m_0$) N_v is calculated to be $7.70\times10^{14}\,T^{3/2}$ cm^{-3} for GaSb. Least-squares fits to the above

TABLE I. Final values of fitting parameters used for modeling hole concentration versus temperature and mobility versus temperature Hall-effect data of an undoped GaSb substrate and OMVPE grown undoped and lightly carbon-doped GaSb epilayers. E_{carbon}, $E_{native1}$, N_{carbon}, N_{native} correspond to the Hall determined activation energies and concentrations of the carbon and native acceptors, respectively. N_D is the donor concentration. μ_{300K} and μ_i are the mobilities of the valence band at 300 K and of the impurity band, respectively.

Sample conditions	E_{carbon} (meV)	$E_{native1}$ (meV)	N_{carbon} (cm^{-3})	N_{native} (cm^{-3})	N_D (cm^{-3})	$A(\mu_{300\ K})$ (cm^2/V s)	α	μ_i (cm^2/V s)
Substrate	NA	19	NA	2.3×10^{17}	3.8×10^{16}	632	1.00	0.01
0 sccm	11	22	1.2×10^{16}	4.2×10^{16}	$<10^{15}$	759	1.27	32
0.05 sccm	8	20	1.5×10^{16}	4.6×10^{16}	$<10^{15}$	707	1.20	35

expression are indicated in Fig. 1 and were obtained by varying E_{carbon}, $E_{native1}$, N_{carbon}, N_{native}, and N_D. The agreement between the experimental and modeled hole concentrations is excellent for temperatures above the impurity conduction region.

We have also fit the data with a model, which includes the second ionizable state of the native acceptor, but find that there is negligible ionization of the second level in the temperature range studied. Table I shows a summary of the fitting parameters obtained for selected samples in this study. It is clear that the activation energy for carrier freezeout is much larger for the substrate than the OMVPE grown epilayers. An excellent fit to the substrate material is obtained by using only a single deep level acceptor energy as expected from the first ionization energies of the GaSb antisite defect and the absence of shallow carbon acceptors. In contrast to the temperature-dependent Hall-effect data for the GaSb substrate, the undoped and carbon-doped epilayers yielded good fits only with an additional shallow level. The two slope behavior indicates the simultaneous presence of deep and shallow acceptors (see Fig. 2). For the epilayer samples, freezeout was observed to occur over a much more limited range, beyond which an increase in apparent concentration was observed due to impurity banding of the $1s$ states. The rapid onset of impurity band conduction prevents the determination of N_D due to the low donor concentrations in the epilayers in comparison to the GaSb substrate. Therefore we only quote upper limits on the estimated donor concentration. For the lowest doped epilayers, the deep level native concentration was found to be significantly higher than the shallow carbon concentration. The activation energies of the specific impurities are not constant but vary depending upon the concentration of impurities. The origin of this effect is discussed below.

In both cases, the lightly carbon-doped GaSb epilayers have fitted values of $N_{carbon}<N_{native}$. This is consistent with the saturation of the hole concentration as a function of CCl_4 flow depicted in Fig. 3. Subtracting a constant native defect concentration from all data points produces a linear relationship, plotted as a solid line in Fig. 3.

The apparent increase of carrier concentration at the lowest temperatures evident in Fig. 1 can be explained by a simple two channel conduction picture. As holes freezeout

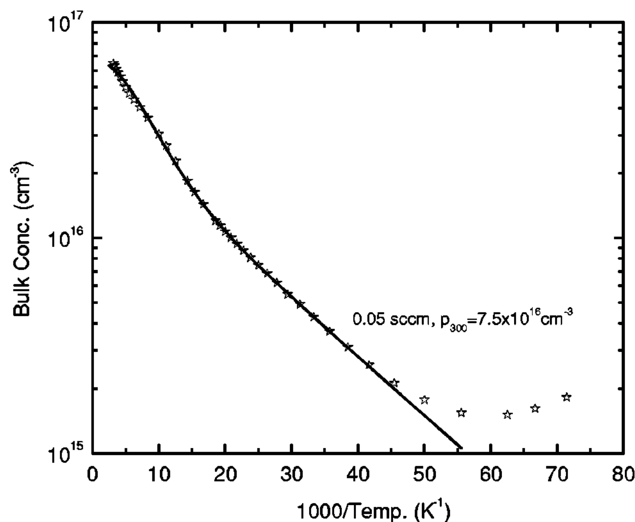

FIG. 2. Expanded view of the temperature-dependent free-carrier concentrations for the 0.05 sccm sample showing the quality of the fit, and the clear two slope behavior caused by the presence of deep and shallow impurities.

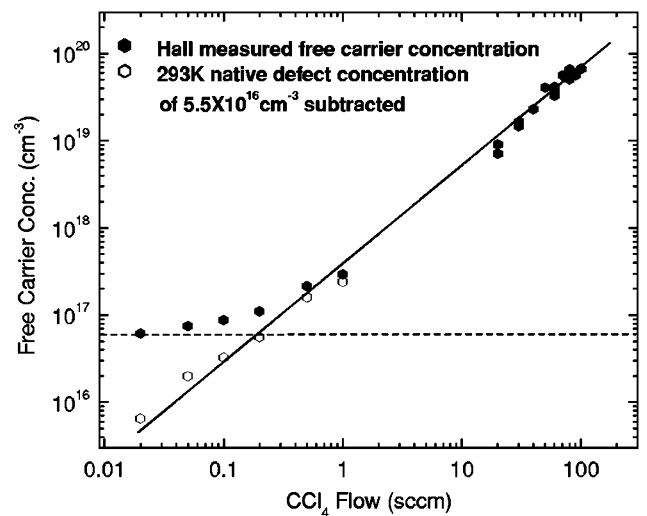

FIG. 3. Hall measured free-carrier concentration as a function of CCl_4 flow. The carbon impurity concentration is determined by subtracting the approximate native defect concentration for OMVPE grown epilayers from the Hall measured free-carrier concentration. The straight line represents a linear fit to the subtracted data.

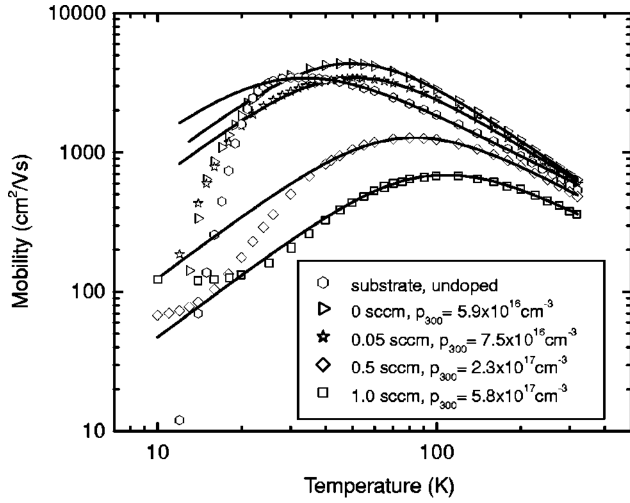

FIG. 4. Temperature-dependent mobility for undoped and lightly carbon-doped GaSb samples. Theoretical fits are denoted by solid lines and take into consideration phonon and impurity as the dominate scattering mechanisms. Divergence of the experimental data from the theoretical fit occurs due to impurity band conduction.

on the $1s$ states, impurity conduction eventually dominates over valence-band conduction, leading to an increase in the apparent carrier concentration. Since the native acceptor level is much deeper than the shallow carbon acceptor level, the amount of overlap of the ground-state orbitals of the native acceptor is expected to be much lower. Hence the freezeout for the substrate sample occurs over several orders of magnitude and impurity conduction is not evident until around 10^{13} cm^{-3}, despite a high hole concentration of around 3×10^{17} cm^{-3} in the substrate material. Even the most lightly carbon-doped samples exhibit more evidence of impurity banding than the substrate material, despite having a substantially lower carrier concentration at room temperature.

The similarity of the freezeout and activation data for the undoped and doped epitaxial samples confirms the presence of a shallow acceptor in the undoped material, likely due to residual carbon from free radicals produced by cracking of the organometallics in the OMVPE process. Typically, the highest quality undoped GaSb epilayers grown by our group contained unintentional carbon doping levels of $N_{carbon} \approx 10^{16}$ cm^{-3}, as determined from hole concentration fits.

Temperature-dependent mobility results for the samples previously shown in Fig. 1 are plotted with theoretical fits in Fig. 4. All OMVPE grown epilayers that are undoped or lightly carbon doped have higher mobilities than the substrate material. The increased mobilities at higher temperatures support the conclusion that the lower hole concentrations observed in the carbon-doped epilayers are not simply due to compensation. In contrast, Johnson *et al.* report that MBE grown GaSb epilayers, with the lowest residual acceptor concentrations, do not display the highest mobilities, as a result of compensation effects.[16]

A simple mobility fit was made assuming that the main scattering mechanisms are due to ionized impurity and phonon mechanisms. Nondegenerate phonon scattering in general is of the form[17]

$$\mu_{lat}(T)=\mu_I\left(\frac{300}{T}\right)^{\alpha}, \tag{3}$$

where μ_I is the mobility at 300 K, α is a constant that is taken to be 1.5 for spherical parabolic bands, and T is the temperature. Ionized impurity scattering is commonly assumed to vary as[17]

$$\mu_{II}(T)=A\left(\frac{T}{300}\right)^{3/2}, \tag{4}$$

where A is a constant and T is the temperature. The two scattering mechanisms are summed according to Mathiesen's rule,

$$\frac{1}{\mu}=\frac{1}{\mu_{lat}}+\frac{1}{\mu_{II}}. \tag{5}$$

Although this is a crude approximation, it highlights the general scattering mechanisms in the mobility data. Least-squares fits using A and α as variable parameters are shown as solid curves in Fig. 4. The agreement between experimental data and phonon scattering predicted by Eq. (5) for higher temperatures is excellent. The final parameters of A and α are reported for each fit in Table I. At lower temperatures the experimental data decrease much more rapidly than predicted by the ionized impurity $T^{3/2}$ slope. The temperature of this divergence in the mobility data coincides almost exactly with the onset of impurity band behavior in the carrier concentration data. Taking impurity banding into consideration the Hall mobility for the case of two carrier conduction is given by[15]

$$\mu_H=\frac{p_v\mu_v^2+p_i\mu_i^2}{p_v\mu_v+p_i\mu_i}, \tag{6}$$

where p_v and p_i are the hole concentrations in the valence band and impurity band and μ_v and μ_i are the mobilities of the valence band and impurity band. Fits using this model on the GaSb substrate and undoped OMVPE grown GaSb epilayer are shown in Fig. 5. Also plotted for comparison as dashed lines are fits using Eq. (5) and reported previously in Fig. 4. The impurity band mobility μ_i is assumed to be temperature independent. Values of μ_i are reported in Table I. It is expected that the overlap of the $1s$ states of the deep level acceptors in the substrate is small due to the small Bohr radii for these states. This is confirmed by an impurity channel mobility of $\mu_i \approx 0$ needed to fit the substrate experimental data. In contrast the 1s orbitals of the carbon acceptors are more delocalized leading to increased banding and hence a higher impurity band mobility of $\mu_i \approx 30$ cm^2/V s. For the highest doped sample in Fig. 4 with a CCl_4 flow of 1 sccm and an estimated carrier concentration of 5.8×10^{17} cm^{-3}, the limiting impurity band mobility is roughly 100 cm^2/V s, indicating significant impurity banding, approaching degenerate conduction.

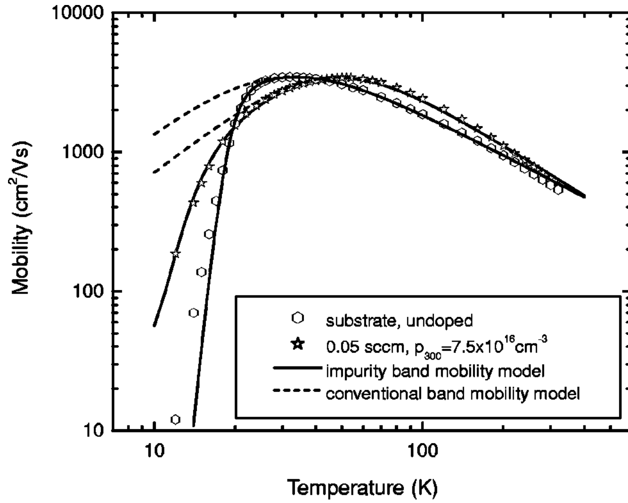

FIG. 5. Selected theoretical fits to the GaSb substrate and lightly carbon-doped GaSb epilayer taking into account impurity band conduction. The dashed line is the same fit as shown in Fig. 4 and only takes into consideration phonon and impurity scattering. The solid line assumes the dominant mechanisms at high temperatures are phonon and impurity scattering whereas at low temperatures a constant low mobility impurity band channel dominates.

B. Photoluminescence analysis

Figure 6 shows low-temperature PL spectra from GaSb/GaSb (001) layers with varying CCl_4 flows. The top-most curve is a reflectance spectrum of the unintentionally

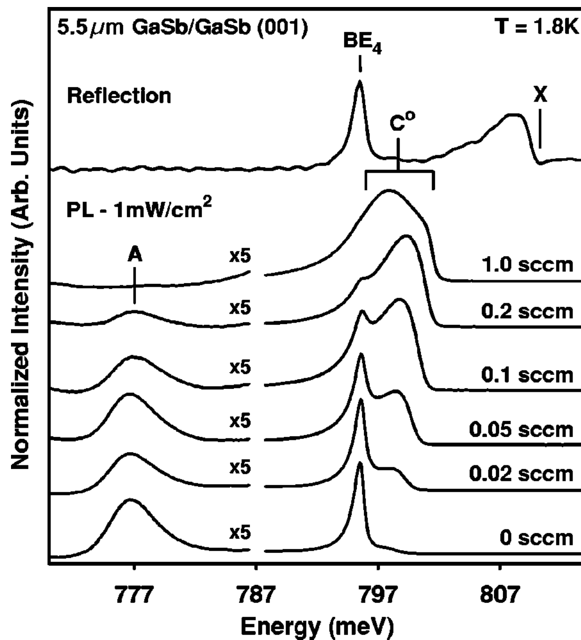

FIG. 6. The top curve is reflectivity from an unintentionally doped GaSb layer showing the reflectivity feature of the free exciton (X). The remaining spectra are low excitation PL of unintentionally and intentionally C-doped GaSb OMVPE layers. Carbon incorporation for each sample is shown by the CCl_4 flow on the right. PL curves on the low-energy side of the break are scaled as indicated.

p-doped sample. It exhibits a free-exciton (X) reflectance feature at 810.2 meV together with bound exciton (BE_4) luminescence at 795.5 meV resulting from the white light illuminating the sample. The free exciton energy, in conjunction with its binding energy [1.4 meV (Ref. 18)], yields a band gap of 811.6 meV, which agrees very well with previously published values.[19–22] The BE_4 luminescence feature is accepted to be the bound exciton related to the native acceptor caused by the double defect V_{Ga}-Ga_{Sb}. The *A* line has been attributed to either DAP or FB luminescence, associated with the first neutral state of the native acceptor.[23] The feature labeled $C°$ increases in intensity for increasing carbon doping levels and is attributed to PL involving holes bound to neutral carbon acceptors. This feature was reported previously by us in samples grown on GaAs substrates, where the features were redshifted by 2.5 meV due to residual strain.[5] The excitation level was kept to a minimum so that this peak would not be confused with shallow bound excitons that have been reported in other experiments.[19,20,24] The $C°$ feature has two possible explanations: DAP or FB recombination. In previous literature on the PL of GaSb, there has been little decisiveness on whether acceptor related transitions are FB or DAP transitions. Because of the high concentrations of the native defect in typical GaSb layers, acceptor-related PL lines in GaSb are broad and lack distinctive features needed for conclusive identification. The small donor binding energy (equal to 2.3 meV using the hydrogenic donor model) complicates the discrimination between the two transitions. Referring back to Fig. 6, the $C°$ feature monotonically broadens with increasing carbon concentration, and the peak energy initially blueshifts 1.5 meV with increasing doping and subsequent redshifts at high carbon incorporation. In comparison, the *A* line does not experience a peak shift, and its width remains relatively constant. Because both the native and carbon acceptor PL should have similar contributions from electrons (either from free electrons in the conduction band or donor bound electrons), the effect of the broadening of the $C°$ peak must originate in the carbon acceptor levels. The blueshift can be explained by associating the $C°$ peak with a DAP transition. As the carbon concentration is increased, the average carbon-donor distance is reduced, which results in an increase of the Coulomb term for the DAP luminescence energies. By increasing the Coulomb term, the peak will shift to higher energies. From the temperature-dependent Hall-effect measurements on samples grown on GaAs substrates under identical conditions, we estimate the carbon concentrations of the undoped sample and the 0.1-sccm sample to be approximately 1×10^{16} cm^{-3} and 6×10^{16} cm^{-3}, respectively. The Hall-effect data indicate that the donor concentrations are much lower than the acceptor concentrations, therefore the average pair separation is no greater than the average acceptor concentration, and can be approximated as $r_{pair} \approx N_A^{-1/3}$. The Coulomb shift is given by

$$\Delta E = \frac{e^2}{4\pi\varepsilon_o\kappa}\left(\frac{1}{r_1} - \frac{1}{r_2}\right), \tag{7}$$

where κ is the dielectric constant of 15.7 at 300 K, r_1 and r_2 are the average pair separations at the two doping limits in

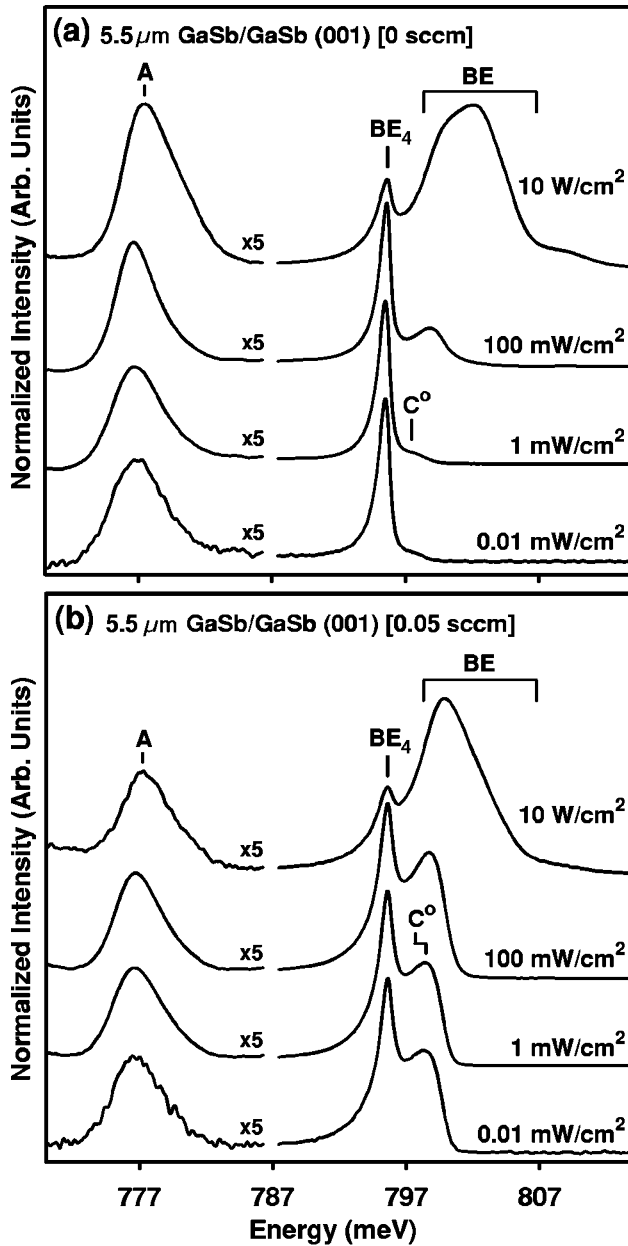

FIG. 7. Low-temperature ($T = 1.8$ K) PL spectra of a GaSb layer with increasing excitation densities for: (a) unintentionally doped sample and (b) moderately doped sample. Ar^{+} laser excitation densities are shown on the right. PL curves on the low-energy side of the break are scaled as indicated.

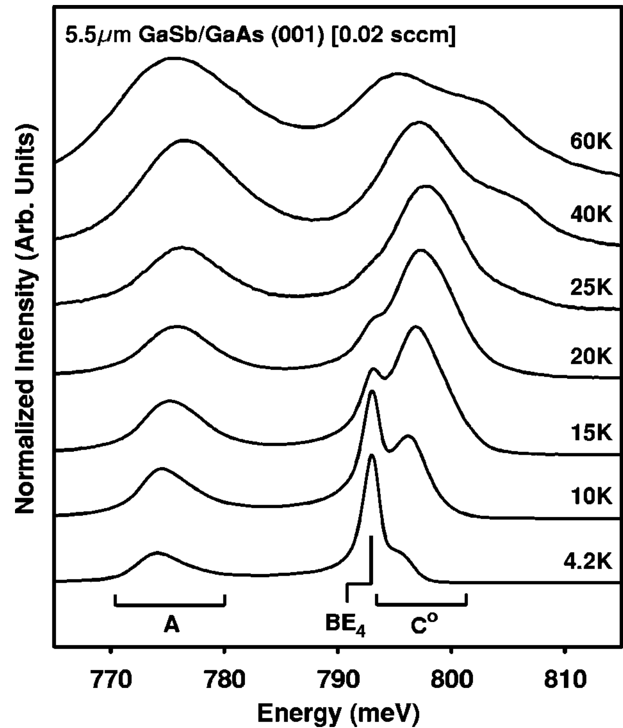

FIG. 8. Temperature-dependent PL of the lowest intentionally C-doped GaSb/GaAs layer ($CCl_4 = 0.02$ sccm). The PL features are shifted down in energy by ≈ 1.3 meV with respect to the homoepitaxial layers because of the strain induced by growing on the GaAs substrate.

Fig. 6. Assuming the range of acceptor concentrations above and calculating the respective pair separations gives $\Delta E \approx 1.5$ meV which is in agreement with the observed PL peak shift. The peak of a FB transition should either remain constant with increasing doping[25] or redshift at high acceptor concentrations resulting from broadening of acceptor impurity levels into the valence band and subsequently causing band-gap narrowing.[26] The redshift of the C° peak at very high acceptor concentrations is attributed to band-gap narrowing.

Figure 7 shows the intensity dependence of the spectra from (a) the undoped sample and (b) a moderately carbon-doped sample, with an excitation density range of six orders of magnitude. Apart from a change in the signal-to-noise ratio, the spectra in each of the two lowest excitation densities are identical for both samples. We postulate that both of these excitation densities are in a low excitation limit, where increasing the number of carriers does not significantly alter the average donor-acceptor separation during DAP recombination. The A line does not show an appreciable peak shift, but in both samples, it has narrowed which indicates a DAP origin. The C° line has increased in intensity and shifted to higher energy. When the excitation level is increased to 10 W/cm^2, a very intense peak emerges on the high-energy side of the BE_4 luminescence. This is attributed to the bound exciton (BE) lines that have been previously studied.[19,20,24] The BE luminescence overlaps with the C° feature resulting in the inability to properly characterize the C° transition. Since the C° and A lines have similar origins, they should respond similarly to the experimental conditions. At the highest power density, the peak of the A line has shifted by approximately 1 meV. This suggests that the carrier concentration has increased sufficiently to favor recombination of smaller donor-acceptor separations than in the low excitation limit.

Figure 8 shows the temperature-dependent PL spectra of the lowest intentionally carbon-doped GaSb/GaAs (001) layer. Qualitatively, the spectra are very similar to the homoepitaxial samples; they include the C°, A, and BE_4 luminescence peaks with comparable relative intensities. The PL lines are slightly broader than in the homoepitaxial samples

and are shifted to lower energy as a result of the strain from growing on a lattice mismatched substrate.[5] The undoped epilayer has very similar temperature-dependent data to that of Fig. 8, indicating a similar PL peak but with somewhat reduced C° intensity. This is in agreement with the previously presented Hall effect data which showed the presence of a shallow acceptor. This implies that the GaSb OMVPE layers possess residual carbon acceptor concentrations comparable to the concentration of native acceptors as previously indicated by the Hall-effect data. Although the absolute carbon concentrations may vary in other OMVPE grown GaSb samples, analysis of the epitaxial layers should not disregard the contributions from unintentional shallow carbon acceptors.

Figure 8 shows that when the temperature is increased above 4.2 K, the peaks of the A and C° lines both blueshift with the initial increase in temperature and redshift at higher temperatures. By interpreting the A and C° peaks as DAP transitions at low temperatures, the large peak shift can be explained through the evolution of the DAP transition into a FB transition as previously discussed by Wu and Chen.[23] Because of the small donor binding energy coupled with the broad nature of the transitions, the difference between the two transitions is not distinct. As the temperature is raised, the luminescence of the DAP contribution subsides while the FB portion increases in intensity. At the higher temperatures, the transition is entirely FB as all of the donors are ionized. Once the transition from DAP to FB is complete, band-gap shrinkage resulting from increasing the sample temperature causes the eventual redshift in the peak positions. The BE_4 line quickly disappears at higher temperatures because excitons cannot bind due to the large thermal kinetic energy of the electrons and holes. The high-energy peak that appears at the highest temperatures shown results from band-to-band transitions (recombination of free electrons and holes).

To quantify the peak shift of the A and C° lines, their peak energies (relative to 1.8-K values) are presented in Fig. 9. A clear break in the slope of the data suggest a transformation from one physical process to another. To discern between peaks where overlap occurs (in particular, between BE_4 and C°), the spectra have been fit empirically using a linear combination of Gaussian and Lorentzian functions, and the desired peak was isolated to extract peak parameters. Figure 9 also includes three lines indicating possible origins to the peak shift. The solid line represents the predicted peak position that would be expected from an ideal FB transition. This is calculated by adding a correction of $\frac{1}{2}k_BT_e$ to the temperature-dependent band-gap narrowing which results from the typical theoretical treatment of FB transitions provided by Eagles.[25,27] T_e is the electronic temperature, but was taken to be equal to the experimental lattice temperature (T) for this curve. The band-gap change is evaluated using the Varshni equation and recent parameters by Ghezzi *et al.*[21] Assuming that the PL line shape is composed of DAP contributions at low temperature and FB luminescence at high temperatures, the dotted line combines the above band-gap narrowing and FB correction with a linear increase of the peak position of 2.3 meV (the donor binding energy) as the temperature is increased from 0 to 27 K, where the thermal

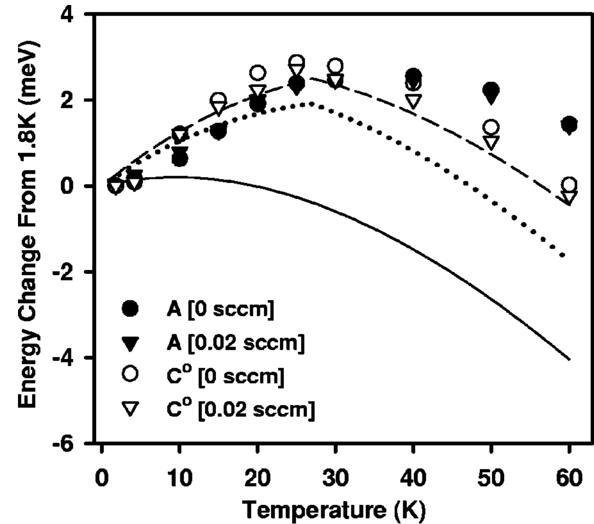

FIG. 9. A and C° peak energies for the GaSb/GaAs samples with CCl_4 flows of 0 and 0.02 sccm. The energies are presented relative to the 1.8-K values. The solid line represents the band-gap change with temperature and includes a $\frac{1}{2}k_BT_e$ correction. The dotted line is calculated using the thermal band-gap contraction, a $\frac{1}{2}k_BT_e$ correction, and a 2.3-meV correction that linearly increases from 0 to 27 K. The dashed line is similar to the dotted line except that the temperature used for the $\frac{1}{2}k_BT_e$ correction uses an electronic temperature 50% larger than the lattice temperature. The temperature-dependent band-gap change is calculated by using the Varshni parameters $a=186$ and $b=0.453$ from Ref. 21.

energy of the electrons is comparable to the donor binding energy. The dashed line is similar to the dotted line but the electronic temperature is assumed to be 50% higher than the lattice temperature. Because of the large impurity concentration in the samples, the electrons are not expected to thermalize to the lattice temperature. While the pure FB description does not explain the large peak shift, the crude approximation of the DAP transforming into a FB transition is much closer to reproducing the temperature-dependent peak positions.

After having determined the origin of the acceptor related transitions, approximate acceptor binding energies can be determined. For DAP recombination, the Coulomb field is zero when the interacting donor and acceptor atoms are infinitely far apart. In this situation, the energy difference from the PL luminescence to the band gap is exactly the sum of the donor and acceptor binding energies. This energy on the DAP transition corresponds to the lowest emission energy of the peak. To experimentally define this point, a linear extrapolation of the low-energy edge of the DAP was performed to zero intensity. Using this fitting procedure to find transition energies for the lowest carbon-doped GaSb homoepitaxial sample, the binding energy for the native and carbon acceptors can be calculated. For the C° transition, the transition energy is 796.2 meV. Using the aforementioned GaSb band-gap of 811.4 meV and donor binding energy of 2.3 meV, the binding energy of the carbon acceptor is found to be 12.9 ± 1 meV. This is similar to the energy that was previously determined for GaSb/GaAs,[5] and to Baldereschi and Lipari's effective-mass calculation of 12.5 meV.[8] The transition energy of the

native acceptor is 773.4 meV resulting in a binding energy of 35.7±1 meV which is consistent with previous results.[9,28]

The spectroscopic ionization energy of the singly charged state of the native defect of 35.7±1 meV deduced from PL is greater than the Hall determined values of 19–22 meV for all samples in this study. Similarly, the observed shallow activation energies of 8–11 meV reported for the undoped and lightly carbon-doped samples are lower than the carbon spectroscopic binding energy of 12.9±1 meV. This well-known reduction in thermal binding energies is due to banding of the acceptor excited states.[29] Similar effects were also observed in lightly carbon-doped GaAs.[18,30] From the data of Baldereschi and Lipari, the Bohr radius for the $2s$ acceptor excited states of GaSb is around 196 Å. This implies that concentrations above roughly 3×10^{15} cm^{-3} the acceptor excited states should be strongly banded, and should merged with the valence band, resulting in the observed reduction in the thermal ionization energy. It is reasonable to expect that the excited states of the first ionized level of the deep antisite defect should not be too strongly perturbed by the central cell effect, and therefore should be close to the effective-mass values. Therefore the same type of excited state banding effect is expected for the native acceptor. In contrast, the $1s$ ground state of the native acceptor is expected to be much more localized than the effective-mass carbon acceptor, resulting in appreciably less impurity banding than for the carbon acceptor level, as shown by the mobility data. Some previous reports on GaSb have used spectroscopically determined binding energies to reduce the number of fitting parameters in their Hall analysis.[13] The present work shows that this is clearly not warranted.

IV. CONCLUSION

We have performed detailed temperature-dependent Hall-effect and PL measurements on a series of samples lightly doped with carbon. Taken together, the Hall-effect and PL data provide a consistent picture of the role of deep and shallow acceptors in undoped GaSb and lightly carbon-doped GaSb films. A shallow carbon related PL band has been identified and attributed to a combination of donor-acceptor pair and free-to-carbon acceptor luminescence. We find the binding energy of carbon acceptors at low temperatures is 12.9±1 meV, which is very close to the effective-mass value estimate. Hall-effect data show thermal ionization energies which approach the spectroscopic value as the impurity concentration is lowered. This behavior was attributed to banding of the $2s$ excited states of the acceptors. We find that the presence of carbon, even at levels lower than the background native defect acceptor concentration has a dramatic effect on the freezeout behavior. Impurity banding of the $1s$ ground states results in a sharp reduction of the mobility below 20 K, which coincides with an increase in the carrier concentration in the limit of low temperatures due to the formation of an impurity band. This effect is strongest in the more heavily carbon-doped samples and weakest in the substrate samples, which are dominated by deep level native impurities.

ACKNOWLEDGMENTS

We acknowledge the support of the Natural Sciences and Engineering Council of Canada (NSERC).

*Electronic address: simonw@sfu.ca

[1] C. R. Bolognesi and S. P. Watkins, Compound Semicond. **6**, 94 (2000).
[2] A. Milnes and A. Y. Polyakov, Solid-State Electron. **36**, 806 (1993).
[3] M. Weyers, N. Putz, H. Heinecke, M. Heyen, H. Luth, and P. Balk, J. Electron. Mater. **15**, 57 (1986).
[4] B. T. Cunningham, M. A. Haase, M. J. M. Collum, J. E. Baker, and G. E. Stillman, Appl. Phys. Lett. **54**, 1905 (1989).
[5] R. D. Wiersma, J. A. H. Stotz, O. J. Pitts, C. X. Wang, M. L. W. Thewalt, and S. P. Watkins, J. Electron. Mater. **30**, 1429 (2001).
[6] J. M. V. Hove, P. P. Chow, M. F. Rosamond, G. F. Carpenter, and L. A. Chow, J. Vac. Sci. Technol. B **12**, 1200 (1993).
[7] X. K. Chen, R. D. Wiersma, C. X. Wang, O. J. Pitts, C. Dale, C. R. Bolognesi, and S. P. Watkins, Appl. Phys. Lett. **80**, 1942 (2002).
[8] A. Baldereschi and N. O. Lipari, Phys. Rev. B **9**, 1525 (1974).
[9] A. N. Baranov, P. E. Dyshlovenko, A. A. Kopylov, and V. V. Sherstnyev, Solid State Commun. **74**, 429 (1990).
[10] W. Jakowetz, D. Barthruff, and K. W. Benz, Inst. Phys. Conf. Ser. **33a**, 41 (1977).
[11] K. Hjelt and T. Tuomi, J. Cryst. Growth **170**, 794 (1997).
[12] P. S. Dutta and H. L. Bhat, J. Appl. Phys. **81**, 5821 (1997).
[13] P. S. Dutta, V. Prasad, and H. L. Bhat, J. Appl. Phys. **80**, 2847 (1996).
[14] R. A. Noack, W. Ruhle, and T. N. Morgan, Phys. Rev. B **18**, 6944 (1978).
[15] H. Fritzsche, Phys. Rev. **99**, 406 (1955).
[16] G. R. Johnson, B. C. Caventt, T. M. Kerr, P. B. Kirby, and C. E. C. Wood, Semicond. Sci. Technol. **3**, 1157 (1988).
[17] M. Balkanski and R. F. Wallis, *Semiconductor Physics and Applications* (Oxford University, New York, 2000).
[18] M. H. Kim, S. S. Bose, B. J. Skromme, B. Lee, and G. E. Stillman, J. Electron. Mater. **20**, 671 (1991).
[19] M. Lee, D. J. Nicholas, K. E. Singer, and B. Hamilton, J. Appl. Phys. **59**, 2895 (1986).
[20] S. C. Chen and Y. K. Su, J. Appl. Phys. **66**, 350 (1998).
[21] C. Ghezzi, R. Magnanini, A. Parisini, B. Rotelli, L. Tarricone, A. Bosacchi, and S. Franchi, Phys. Rev. B **52**, 1463 (1995).
[22] J. Novak, S. Hasenohrl, M. Kucera, K. Hjelt, and T. Tuomi, J. Cryst. Growth **183**, 69 (1998).
[23] M. C. Wu and C. C. Chen, J. Appl. Phys. **72**, 4275 (1992).
[24] W. Ruhle, W. Jakowetz, C. Wolk, R. Linnebach, and M. Pilkuhm, Phys. Status Solidi B **73**, 255 (1976).
[25] K. D. Glinchuck, N. M. Litovchenko, A. V. Prokhorovich, and O. H. Stril'chuk, Semiconductors **35**, 384 (2001).
[26] S. I. Kim, M. S. Kim, S. K. Min, and C. Lee, J. Appl. Phys. **74**, 6128 (1993).
[27] D. M. Eagles, J. Phys. Chem. Solids **16**, 76 (1960).
[28] W. Jakowetz, W. Ruhle, K. Breuninger, and M. Pilkuhn, Phys. Status Solidi A **12**, 169 (1972).
[29] G. E. Stillman and C. M. Wolfe, Thin Solid Films **31**, 69 (1976).
[30] S. P. Watkins and G. Haacke, Appl. Phys. Lett. **59**, 2263 (1991).